Colloid Polym Sci (2009) 287:969–977
DOI 10.1007/s00396-009-2053-9

ORIGINAL CONTRIBUTION

Effective encapsulation of Sudan black B with polystyrene using miniemulsion polymerization

Xiao Zhao · Shuxue Zhou · Min Chen · Limin Wu

Received: 18 February 2009 / Revised: 17 April 2009 / Accepted: 12 May 2009 / Published online: 28 May 2009

Abstract In this study, polystyrene (PS)/Sudan black B (SDB) latex particles were prepared using a miniemulsion polymerization technique in the presence of methyl isobutyl ketone (MIBK). Effects of the weight ratio of MIBK/styrene (St) and the SDB load on the morphology of latex particles and encapsulation efficiency were studied. It was found that the encapsulation efficiency of SDB with PS increased as the weight ratio of MIBK/St rose. The PS/SDB latex particles have a perfect core-shell structure and as high as more than 90% of encapsulation efficiency at 1:1 of MIBK/St. UV irradiation experiments and dynamic light scattering tests indicated that the obtained PS/SDB latexes exhibited excellent photostability and storage stability.

Keywords Sudan black B · Encapsulation · Miniemulsion polymerization · Polystyrene · Core-shell structure

Introduction

Since organic dyes have the advantages of broad color range, great color strength, diverse optical, and electro-optical properties, they have found wide use in laser materials [1]; optical disks [2]; nano-scale semi-conductor devices [3]; and colorants for textile products, inks, and coatings [4, 5]. To meet the development of advanced materials and devices, the optimization of the properties of organic dyes has been gathering great attention in recent years, and numerous researches have been carried out with encapsulation strategies [6, 7]. For example, rhodamine dyes have been embedded into a silica matrix or Si–Ti binary oxide matrix via a sol–gel method to enhance their fluorescent intensity and photostability [8–17]. Pseudoisocyanine dyes have been encapsulated into hollow polyelectrolyte shells using controlled precipitation method and achieved higher photostability[18, 19]. Besides high photostability, better waterproofness and water-dispersibility of organic dyes are also desired when they are used in waterborne systems, such as waterborne inks and coatings. Although water-soluble dyes possess excellent dispersibility in water, they are easily leachable. Oil-soluble dyes, with better waterproofness would be an ideal alternative, but their poor water-dispersibility needs further improvement.

Encapsulation of oil-soluble dyes into polymer latex particles via emulsion polymerization [20, 21], interfacial polymerization [22], and miniemulsion polymerization [23–27] are generally employed to improve water-dispersibility, and the end products are usually named as colored latex. Among these methods, miniemulsion polymerization is much more attractive because of its wide adjustment of particle size (from several tens to several hundred nanometers), low surfactant concentration and high dye load. For instance, Takasu et al. [24, 25] encapsulated copper phthalocyanine dye and styryl dye into polystyrene (PS) latex using miniemulsion polymerization to get colored latex particles with high dye load (30–40 wt%). Hu et al. [26, 27] produced a set of so-called nanocolorants consisting of cross-linked PS with solvent yellow, red, or blue dyes via a modified miniemulsion polymerization process. For all the above cases, the dyes have good solubility in monomers, which is attributed to the successful preparation of colored latex. However, as

X. Zhao · S. Zhou · M. Chen · L. Wu (✉)
Department of Materials Science and Advanced Coatings Research Center of the Ministry of Education of China, Advanced Materials Laboratory, Fudan University, Shanghai 200433, People's Republic of China
e-mail: lmw@fudan.edu.cn

for those oil-soluble dyes with poor solubility in monomers, their improvement of the water-dispersibility (or in other words, preparation of colored latex) via miniemulsion polymerization are seldom involved.

In this article, Sudan black B (SDB) was employed as the typical oil-soluble dye with poor solubility in monomers such as styrene. PS/SDB colored latexes with high encapsulation efficiency were obtained via miniemulsion polymerization in the presence of methyl isobutyl ketone (MIBK), a good solvent for SDB. Effects of the MIBK/styrene (St) weight ratio and SDB load on the encapsulation efficiency and the morphology of the latex particles were investigated. Not only were homogeneous and stable PS/SDB latexes with SDB load as high as 50 wt% successfully fabricated, but the photostability of the SDB dye was also enhanced.

Experimental section

Materials

SDB (C.I.26150, analytical grade, chemical structure shown in Fig. 1), St, 2,2′-azobis(isobutyronitrile) (AIBN), sodium lauryl sulfate (SLS), MIBK, and tetrahydrofuran (THF, analytical grade) were obtained from Sinopharm Group Chemical Reagent (Shanghai, China) and used as received, except for St, which was distilled under reduced pressure before use. Hexadecane (HD) was obtained from Fluka and used as received. Deionized water was used as continuous phase for each polymerization.

Phase partition of SDB between water and St/MIBK phases

In order to examine the role of MIBK in the polymerization processes, the phase partition of SDB in water and oil phase was first tested with or without MIBK. Then, 0.5 g of SDB was charged into 5 g of St or into 5 g of the mixture of St/MIBK with weight ratios changing from 5:1 to 5:5. The obtained mixtures were further added into 40 g water with vigorously stirring. Obvious water/oil phase separation generally occurred after 5 h equilibrium. Two milliliters of liquid was decanted from the water phase and underwent visible absorption measurement using a UV-visible spectrophotometer (UV 1800 PC, Shanghai Meipuda, Shanghai, China).

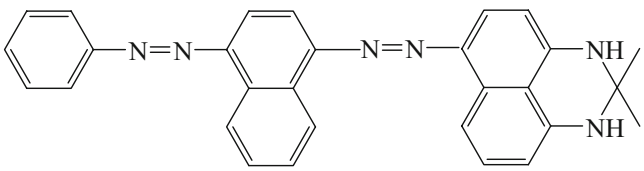

Fig. 1 The chemical structure of SDB

Polymerization

The bare PS latex and the dye-loaded PS latexes were prepared by miniemulsion polymerization according to the recipes in Table 1. The typical process was carried out as follows: various amounts of SDB, 5 g of St, and 100 mg of AIBN with or without 200 mg of HD were mixed as the oil phase, and then added to the aqueous phase, consisting of 400 mg of SLS and 40 g of water, under vigorous stirring. After the mixture was stirred for 1 h, the miniemulsification was obtained by ultrasonicating for 12 min at 70% amplitude using an ultrasonic homogenizer (Scientz Biotechnology, Ningbo, China) with 3-s-pulse on and 3-s-pulse off cycles under ice cooling. The obtained stable miniemulsion was transferred to a reactor and deoxygenated by purging with nitrogen, and then polymerized at 70 °C for about 10 h.

Characterization

UV-visible spectra The absorption spectra were recorded on a UV-visible spectrophotometer (UV 1800 PC, Shanghai Meipuda) at a temperature of 25 ± 1 °C.

Transmission electron microscope observations A transmission electron microscope (TEM, Hitachi H-600, Tokyo, Japan) was used to observe the morphology of pure PS latex and dye-loaded PS latexes. Each sample was dropped onto carbon-coated copper grids and dried at room temperature before examination.

X-ray photoelectron spectroscopy X-ray photoelectron spectroscopy (XPS) analysis was carried out on a PHI-5000C ESCA system. The X-ray source was monochromatic Mg (1,253.6 eV) and powered at 250 W. The survey spectra were collected at a take-off angle of 90° with respect to the sample plane. All the binding energies were calibrated by using the containment carbon (C1s = 284.6 eV). The samples for XPS were prepared as follows: The latex was centrifuged first to obtain the PS/SDB composite particles. These particles were further washed three times with water and vacuum dried overnight at room temperature.

Elemental analysis The PS/SDB composite particles used in XPS analysis were adopted to carry out element analysis using a Elementar Vario EL III CHNS analyzer.

Particle size and its distribution The particle size and its distribution were determined by dynamic light scattering (DLS) using a particle size analyzer (Beckman Coulter, N4

Table 1 Recipes for the synthesis of dye-loaded PS latexes

Latex	Dye (g)	MIBK (g)	HD(g)	Particle size(nm)	PDI
S0	0	0	0.2	88.5	0.038
S1	0.5	0	0.2	_	_
S2	0.5	1	0	185.6	0.328
S3	0.5	3	0	141.3	0.256
S4	0.5	5	0	116.5	0.183
S5	1.0	5	0	121.5	0.243
S6	1.5	5	0	122.6	0.260
S7	2.0	5	0	131.2	0.168
S8	2.5	5	0	148.5	0.242

Five grams of St, 100 mg of AIBN, 40 g of water, and 400 mg of SDS were used for fabrication of all latexes

Plus, Fullerton, CA, USA) at 25 °C with a fixed light incident angle of 90°. Unimodalmode was employed to analyze the data.

Encapsulation efficiency of SDB with PS Diluted SDB/THF solutions with various concentrations were prepared and underwent absorption spectroscopy analysis with a UV-visible spectrophotometer (UV 1800 PC, Shanghai Meipuda). The absorption intensity of the maximum peak (at a wavelength of 600 nm) was plotted as a function of SDB concentration to establish a calibration curve, as shown in Fig. 2. The dye-loaded polymer latexes were ultracentrifuged and washed with ethanol to remove the dissociated dye molecules. The obtained particles were dried overnight in an oven at 80 °C. The dried particles were dissolved in THF based on a concentration of 0.02 mg/ml. Then, the visible spectra of the THF solutions were recorded by the UV-visible spectrophotometer. The actual SDB concentration (C, mg/mL) in THF was obtained from the calibration curve based on the absorption intensity of the maximum peak (at ~600 nm) of the spectrum, and thus, the encapsulation efficiency (E, the mass of SDB inside PS particles dividing the total mass of SDB in the latex) can be calculated as follows:

$$E = \frac{C}{0.02 - C} \cdot \frac{M_{st}}{M_{dye}},$$

where M_{st} and M_{dye} are the weights of St and dye in the recipe in Table 1, respectively.

Photostability The photostability of pure SDB dye and the dye-loaded PS latexes were examined by UV irradiation experiments. SDB/MIBK solution with a concentration of 5×10^{-5} M was prepared. The latex S4 in Table 1 was diluted with water to the same SDB concentration as SDB/MIBK solution. Both samples were placed in a UV crosslinker with five 8-W UV-C tubes (wavelength 365 nm, 3.1 mW/cm^2, Model XLE-1000, Spectroline, Westbury, NY, USA). The absorption spectra were measured as a function of UV irradiation time.

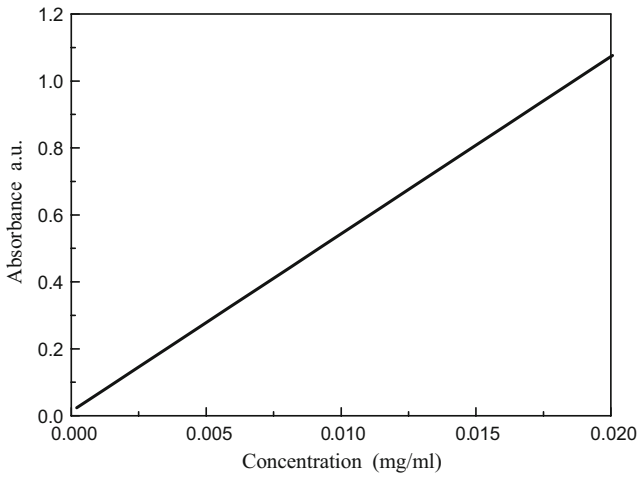

Fig. 2 The maximum absorbance (~600 nm wavelength) of diluted SDB/THF solution as a function of SDB concentration

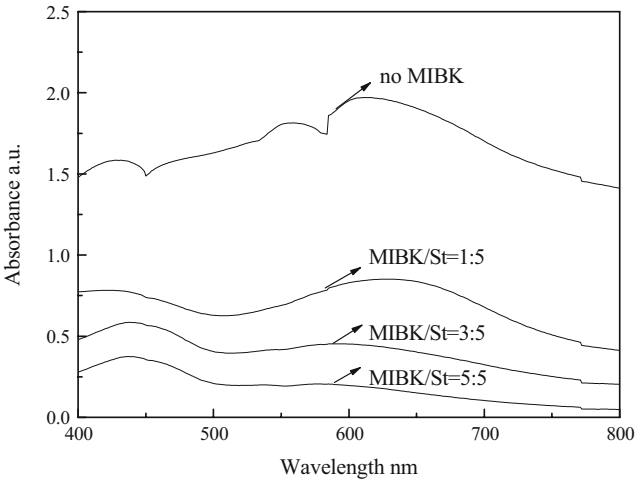

Fig. 3 The absorption spectra of the aqueous phases resulting from the phase separation of the water–St–MIBK–SDB mixtures with different MIBK/St ratios (no surfactant was used in the systems. SDB concentration: 10 wt% based on the total mass of oil phase)

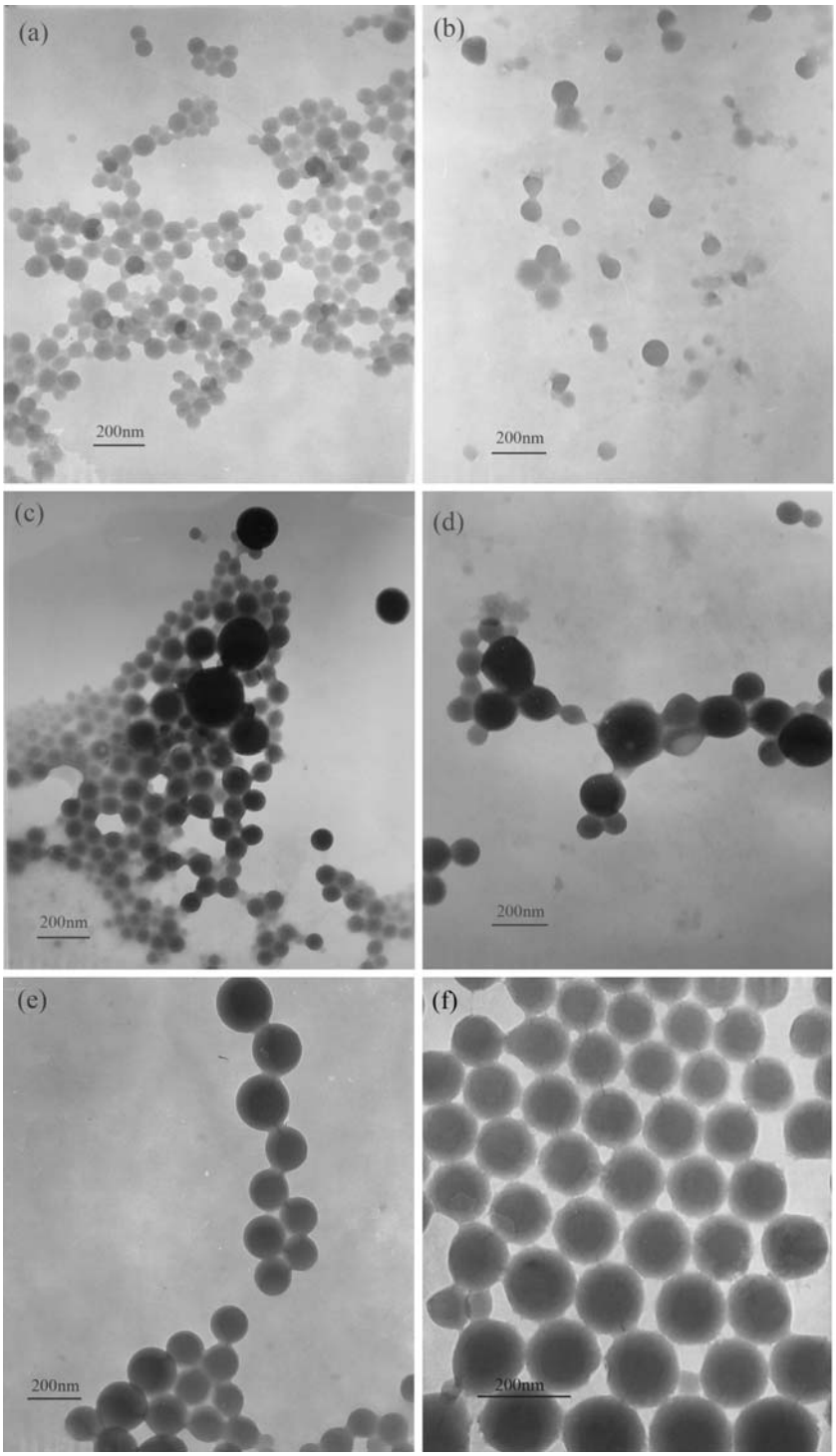

Fig. 4 TEM images of pure and dye-loaded PS latex particles. **a** Pure PS latex particles. **b** S1 (in the absence of MIBK). **c** S2 (MIBK/St 1:5). **d** S3(MIBK/St 3:5). **e** S4 (MIBK/St 5:5). **f** S4 with higher magnification

Results and discussion

Fabrication of PS/SDB latexes

Effect of MIBK/St ratio

With the miniemulsion polymerization method, dispersion or dissolvation of organic dyes in monomer droplets is critical to accomplish the high encapsulation efficiency of organic dyes with polymer [28, 29]. Unfortunately, the SDB dye in this study has only limited compatibility with St; thus, a good solvent, MIBK, was employed to increase the solubility of SDB in monomer droplets. The effect of the MIBK/St ratio on the partition of SDB between water and MIBK/St mixture was examined first by determining the absorption spectra of the aqueous phase in the visible

light range as shown in Fig. 3. It clearly indicates that the absorption intensity in the whole visible light range considerably decreases with increasing amounts of MIBK, suggesting the decline of SDB in the aqueous phase. Three peaks at 428, 559, and 617 nm could be identified in the spectrum of the case without MIBK, which might be ascribed to the formation of dye agglomerates. As for the cases with MIBK, the peak at 559 nm disappears while the peak at 617 nm is gradually changing to be a shoulder as the MIBK/St ratio increases, which also demonstrates the decrement of SDB concentration in aqueous phase. Therefore, the addition of MIBK is beneficial for the transfer of SDB from aqueous phase to oil phase. Additionally, Fig. 3 shows that the absorption intensity reaches zero at a MIBK/St ratio of 5:5, meaning that the MIBK with a half weight of the oil phase is enough to assure the residing of SDB dye in oil phase.

The water–St–MIBK–SDB mixtures with different MIBK/St ratios were miniemulsified by ultrasound in the presence of SLS and further underwent polymerization to obtain PS/SDB latexes. Figure 4 displays the TEM images of the PS/SDB latex (S1–S4) particles; the dye-free PS particles (S0) were also synthesized by miniemulsion polymerization for the sake of comparison. As illustrated in Fig. 4a, the pure PS particles are spherical and monodisperse with a diameter of around 80 nm. Once 0.5 g of SDB (S1 in Table 1) was introduced, both spherical particles with clear boundary and irregular particles with obscure boundary are observed (see Fig. 4b). The spherical particles should be formed from the monomer droplets with/without SDB dye, while the irregular particles might result from the SDB agglomerates in aqueous phase. Being consistent with the spectrum observed in Fig. 3, this result suggests that the SDB dye could not be efficiently encapsulated into PS particles in the absence of MIBK because SDB dye molecules were partly transferred to the aqueous phase and formed dye agglomerates. Figure 4c–f illustrates the effects of MIBK/St weight ratios on the morphology of the produced latex particles. At 1:5 of MIBK/St ratio, the size of the obtained latex particles increases and the centers of the particles are darker compared with those in Fig. 4a and b, which might be attributed to the encapsulation of SDB dye into the PS matrix. However, a few irregular fragments still existed on the surface of partial particles, showing that the SDB dyes are not completely encapsulated into PS particles at 1:5 of MIBK/St ratio. When the MIBK/St ratio further increased to 3:5, the mean particle size of the achieved latexes decreased and the size distribution became narrower (see Fig. 4d–f), which should be ascribed to much more homogeneous dispersion of SDB in oil phase and higher encapsulation efficiency. More interestingly, the particles possess a distinctive core-shell structure at a St/MIBK ratio

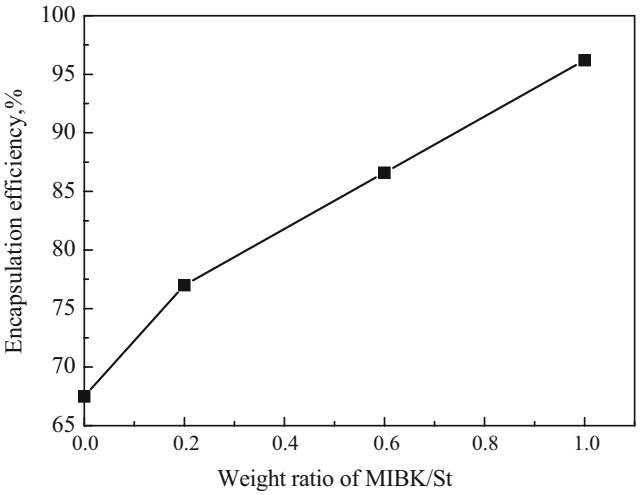

Fig. 5 The encapsulation efficiency of SDB as a function of weight ratio of MIBK/St

of 5:5. As revealed in Fig. 4f, the average thickness of the shell of the prepared latex is more than 20 nm, and the diameter of the core is around 60 nm. This structure may be formed as follows: after the miniemulsification stage, nearly all SDB reside in oil droplets (mixture of St and MIBK) homogeneously with the aid of a constant fusion–fission process. Once polymerization proceeds, the monomer, initial co-solvent of SDB, is consumed gradually and polymerized to be the shell of the achieved latex particles. As a result, the concentration of SDB in the oil phase becomes higher and the dye molecules start to aggregate and ultimately form the core. In addition, the formed dye aggregates can be used as co-stabilizer to impress Ostwald ripening in the following polymerization processes [23].

The average particle size and polydisperse index of the particles were further analyzed by DLS and summarized in Table 1. It can be seen that the particle size decreases and

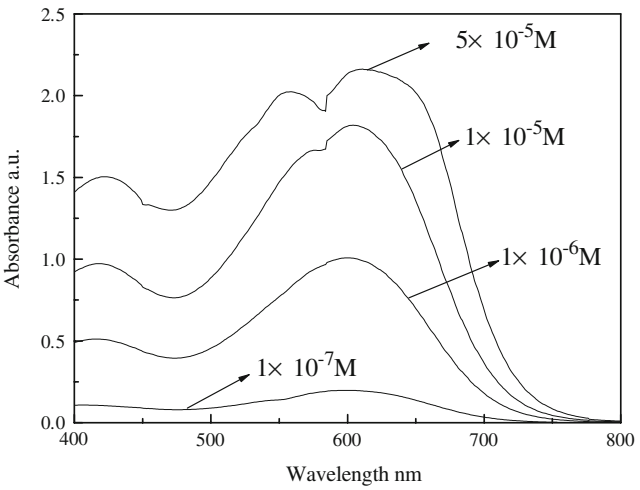

Fig. 6 The absorption spectra of SDB dispersions in the mixture of St and MIBK (MIBK/St = 1:1 wt/wt) at various concentrations

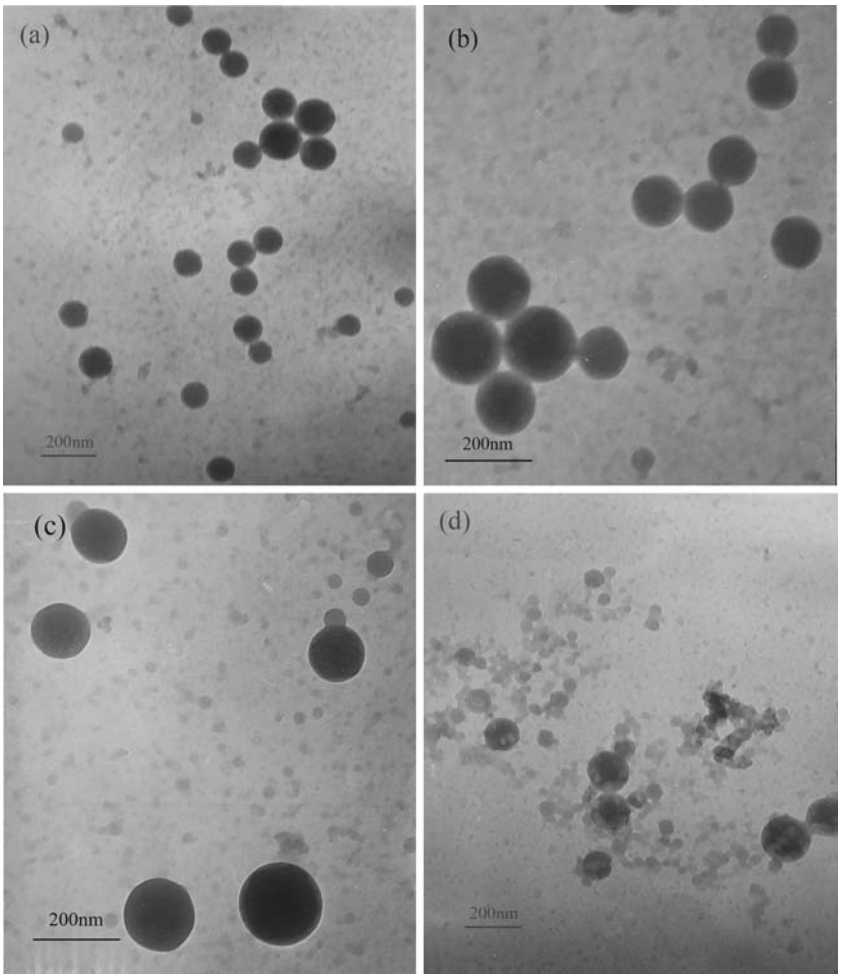

Fig. 7 TEM images of PS/SDB latex particles: **a** S5 (20 wt% SDB), **b** S6 (30 wt% SDB), **c** S7 (40 wt% SDB), **d** S8 (50 wt% SDB)

the particle size distribution narrows as the weight ratio of MIBK/St increases, which is consistent with the TEM results. Figure 5 illustrates the encapsulation efficiency of SDB as a function of the weight ratios of MIBK/St. It could be seen that an encapsulation efficiency as high as 96.2% was actually achieved when the weight ratio MIBK/St was raised to 5:5. This result agrees with absorption spectra of aqueous phase, as shown very well in Fig. 3 and TEM images in Fig. 4.

Effects of SDB concentration

It is well known that organic dyes tend to aggregate, driven by weak noncovalent interactions, including hydrogen bonds, aromatic π stacking, and electrostatic and van der Waal's interactions [30–33]. To understand the architecture of SDB in the binary solvents of MIBK/St (weight ratio: 1:1), which consists of the oil phase in the succedent miniemulsion polymerization, the absorption spectra of SDB dispersions with various concentrations were firstly examined, as shown in Fig. 6. At very low concentrations (1×10^{-7} M) of SDB, a very weak peak at 600 nm and a shoulder at 414 nm are identified, indicating that the SDB exists in the form of monomers. Similarly, when SDB content was increased to 1×10^{-6} M, a peak absorption at around 600 nm and a shoulder at 415 nm are observed, suggesting the SDB aggregates are still absent in the oil phase. However, when the SDB concentration was further increased to 1×10^{-5} M, new peaks appeared at 604 and 571 nm. Meanwhile, the shoulder peak turns into a distinct

Table 2 The *C* and *N* atomic concentrations of S4 and S7 determined from elemental analysis and XPS analysis

Samples	Elemental analysis			XPS analysis		
	C (wt %)	*N* (wt %)	*C*/*N*[a]	*C* (%)	*N* (%)	*C*/*N*[a]
S4	73.97	6.870	12.6	84.68	1.59	53.3
S7	73.99	13.41	6.4	77.92	4.44	17.5

Atomic ratio

peak with a 6-nm red shift. All these changes reveal the formation of SDB trimers and polymers. At a concentration of 5×10^{-5} M (~0.005 wt%), the two peaks shift to 553 and 612 nm, respectively, indicating that SDB aggregates begin to form. In the following fabrication of PS/SDB miniemulsions, SDB concentration changed from 10 to 50 wt% based on the weight of St, which is much higher than 5×10^{-5} M; therefore, the SDB dye in the miniemulsion droplets exist in the form of aggregates.

For practical application, high SDB-loaded PS/SDB miniemulsions would be favorable. The usage of SDB was thus increased from 0.5 to 2.5 g based on the recipes (see S5, S6, S7, and S8 in Table 1). All miniemulsions were rather stable during polymerization, and no agglomerates were observed. The TEM images of the PS/SDB latex particles with different SDB loads are shown in Fig. 7. Large particles with spherical shapes and small particles with irregular shapes coexisted for all samples. These small particles should belong to the dissociated SDB dyes, like the case we observed in Fig. 4b. The fraction of the small particles may be reduced by increasing the amount of MIBK charged. As for the large particles, the core-shell structure can be seen. Compared with Fig. 4e, f, it is found that the more the amount of SDB dye was charged, the thinner the shell of PS/SDB latex particles was.

XPS analysis and elemental analysis were further employed to characterize the structure of the large particles. The results for samples S4 and S7 are summarized in Table 2. The atom, *N*, was probed in XPS analysis for both samples. These *N* atoms could result from the fragments of the initiator, AIBN, and/or SDB dyes. Nevertheless, the *C*/*N* atomic ratio from XPS analysis increased with increasing SDB load (comparison between S4 and S7), indicating the existence of SDB molecules at the surface of the large particles. However, these values from XPS analysis are much smaller than those from elemental analysis, suggesting the SDB dye tends to stay in the core. This fact demonstrates that the core-shell structure is true for the formed PS/SDB composite particles. Table 2 also reveals that the *N* atom fraction of S7 has 2.79 times higher XPS characterization, but only 1.95 times higher elemental analysis relative to the corresponding values of S4. That is, the increasing rate of *N* atoms at the surface of the particles is higher than that of the particles. This result must be attributed to the thinner shell of S7, being consistent with the TEM observation.

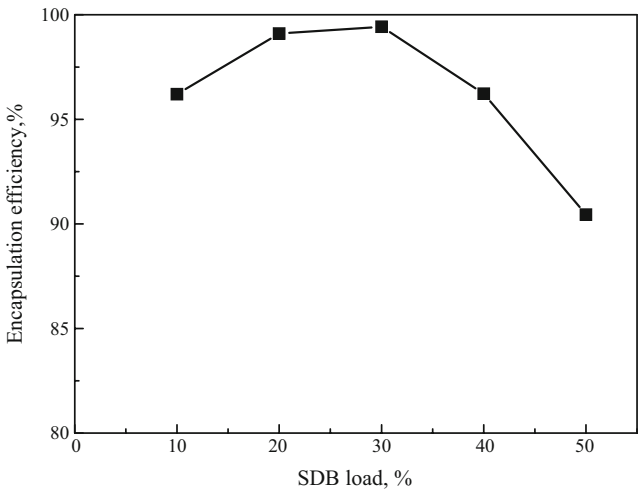

Fig. 8 The encapsulation efficiency of SDB as a function of SDB load

Fig. 9 The appearance of S8 latex

The size and size distribution of the PS/SDB latex with various SDB loads, as summarized in Table 1, basically match the TEM results in Fig. 7. The encapsulation

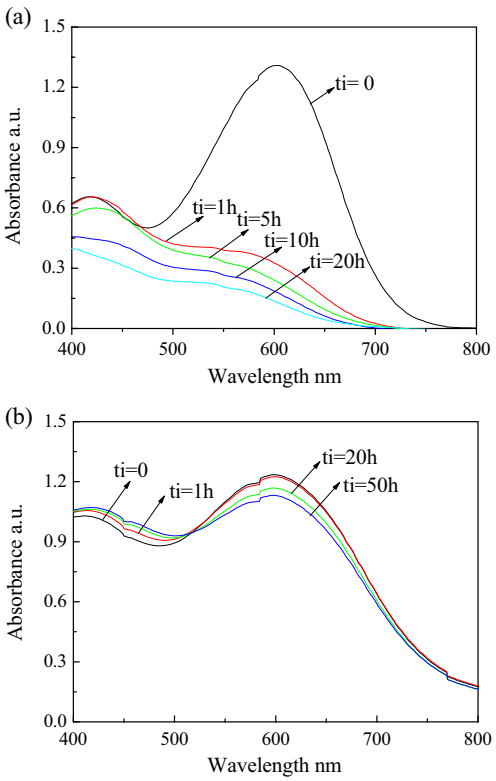

Fig. 10 Absorption spectra of **a** SDB/MIBK solution and **b** S4 latex before and after UV irradiation with different irradiation times (*ti*)

efficiency of SDB as a function of SDB load is plotted in Fig. 8. High encapsulation efficiency over 96% was obtained at SDB load below 40 wt%. However, a relatively low encapsulation efficiency of 90.5% was reached at 50 wt % of SDB load, which is consistent with TEM results. Consequently, SDB dyes could still be expelled from the oil droplets at very high SDB concentrations, even in the presence of MIBK. Nevertheless, it is worth noting that, even when SDB concentration is as high as 50 wt%, this latex is still homogeneous and no flocculates or precipitates are found, as seen by its appearance in Fig. 9.

Photostability of PS/SDB latexes

It is expected that the photostability of dye molecules could be improved via encapsulating them into polymer matrixes. To examine the effect of the encapsulation process on the light fastness of the SDB dye, the latex S4 was taken as an example to undergo UV irradiation. A SDB/MIBK solution with a concentration of 5×10^{-5} M was also carried out for a UV irradiation experiment for the sake of comparison. Figure 10 presents the visible absorption spectra of the SDB/MIBK solution and the latex S4 before and after UV irradiation. Before UV irradiation, the spectrum of SDB/MIBK solution has an absorption peak at ~600 nm and a shoulder at ~415 nm. The absorption intensity of the peak at ~600 nm decreased remarkably just after 1 h of exposure, and almost faded completely after 20 h of UV irradiation. The absorption intensity at the shoulder also declined to a large extent as UV irradiation time extended. However, for the latex S4, the absorption intensity after 1 h of UV exposure was almost the same as before UV irradiation, and only slightly reduced even the irradiation time reached after 50 h. More interestingly, it is found that the intensity at the shoulder (415 nm) slightly increased after the sample was exposed to the UV light. Therefore, the encapsulation of SDB with PS can improve the photostability of the dye considerably.

The enhanced photostability of PS/SDB latex particles can also be revealed from the change in appearance of the samples after UV irradiation, as illustrated in Fig. 11. The color of the SDB/MIBK solution changes to brown from the original black (Fig. 11a), while the color of the latex S4 does not change after UV irradiation (Fig. 11b).

The better photostability of PS/SDB latex particles could be explained by the single-photo photobleaching mechanism. Active singlet oxygen can oxidize a single dye molecule, and this photo-oxidation process mainly causes fading of the dye molecules under UV irradiation. Therefore, all organic dyes exhibit higher photostability in an oxygen-depleted atmosphere. The incorporation of SDB into PS matrix means that the SDB dye molecules are protected from oxygen, and thus, the PS/SDB latex particles exhibit improved photostability. This result further confirms the successful encapsulation of SDB dye into PS particles.

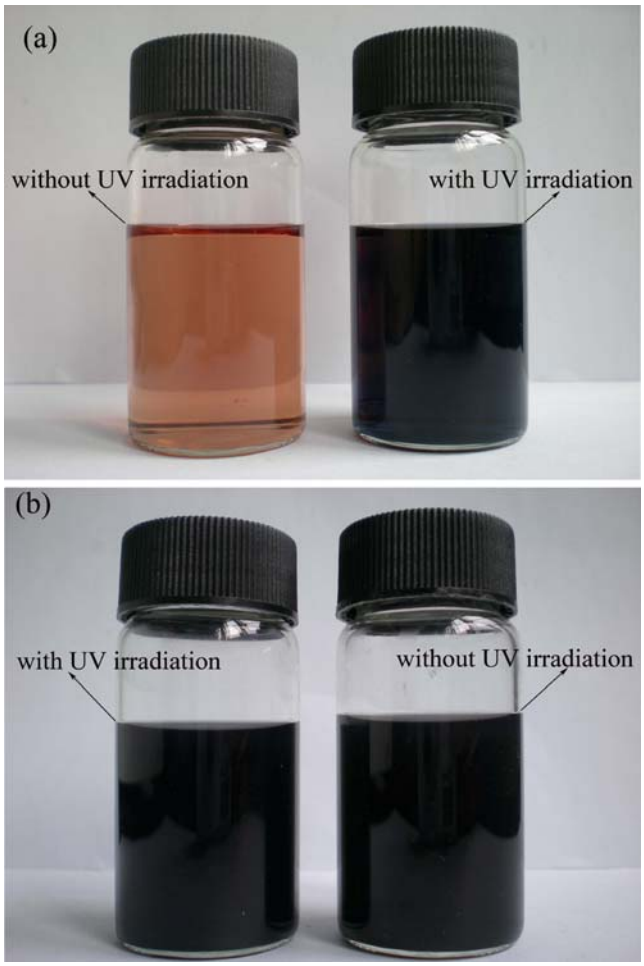

Fig. 11 The appearances of **a** SDB/MIBK solution (5×10^{-5} M) with and without UV irradiation for 20 h and **b** S4 latex (5 × 10−5 M) with and without UV irradiation for 50 h

Storage stability of PS/SDB latexes

DLS was employed to examine the long-term stability of the latexes. Table 3 compares the particle size and size

Table 3 Effect of the storage on the particle size and size distribution of the PS/SDB latexes

Latex	Particle size (nm) As-synthesized latex	PDI	Particle size (nm) After 30days of storage	PDI
S4	116.5	0.183	115	0.142
S5	121.5	0.243	120.1	0.223
S6	122.6	0.260	115.8	0.233
S7	137.6	0.168	131.2	0.15
S8	148.5	0.242	152.7	0.293

distribution of the latexes that were kept for 30 days with those of the as-synthesized latexes. It can be found that the sizes and size distributions of the latexes were almost the same as their initial values. In addition, no precipitates were produced during storage for all PS/SDB latexes. Therefore, the PS/SDB latexes produced herein have very good storage stability.

Conclusions

Water-insoluble SDB dye was successfully encapsulated into PS particles via miniemulsion polymerization. Addition of MIBK in the recipe is beneficial for the residing of SDB in oil droplets, as well as for the stabilization of the miniemulsion. Based on the absorption spectra and the morphology of the latex particles, a MIBK/St weight ratio of 1:1 would be ideal for the fabrication of PS/SDB latex particles. More than 90% of encapsulation efficiency can be attained even at 50 wt% of SDB load. TEM images show that the dye-loaded latex particles possess core-shell structure, and the shell becomes thinner with increasing SDB load. The obtained PS/SDB latexes exhibit excellent photostability and storage stability.

Acknowledgements Financial support for this research from the Foundation of Science and Technology of Shanghai (07DJ14004), the Shanghai Leading Academic Discipline Project (B113), the Shanghai Excellent Leader of Academic Discipline Project, and the Shuguang Scholar-Tracking Foundation of Shanghai is greatly appreciated.

References

1. Lanzafame JM, Muenter A, Brumbaugh DV (1996) Chem Phys 210:79–89
2. Kietzmann R, Ehret A, Spitler M, Willing F (1993) J Am Chem Soc 115:1930–1936
3. Khazraji AC, Hotchandani S, Das S, Kamat PV (1999) J Phys Chem B 103:4693–4700
4. Ozdemir O, Armagan B, Turan M, Celik MS (2004) Dyes Pigm 62:49–60
5. Itoh H (1997) US Patent 5(690):721
6. Chávez JL, Wong JL, Jovanovic AV, Sinner EK, Duran RS (2005) IEE Proc-Nanobiotechnol 152:73–84
7. Arunkumar E, Forbes CC, Smith BD (2005) Eur J Org Chem 2005:4051–4059
8. Monte FD, Levy D (1998) J Phys Chem B 102:8036–8041
9. Ferrer ML, Monte FD, Levy D (2003) Langmuir 19:2782–2786
10. Monte FD, Mackenzie JD, Levy D (2000) Langmuir 16:7377–7382
11. Avnir D, Levy D, Reisfeld R (1984) J Phys Chem 88:5956–5959
12. Gutiérrez MC, Hortigüela MJ, Ferrer ML, Monte FD (2007) Langmuir 23:2175–2179
13. Gilliland JW, Yokoyama K, Yip WT (2004) Chem Mater 16:3949–3954
14. Pouxviel JC, Dunn B, Zink JI (1989) J Phys Chem 93:2134–2139
15. Negishi N, Fujino M, Yamashita H, Fox MA, Anpo M (1994) Langmuir 10:1772–1776
16. Bujdák J, Iyi N (2006) J Phys Chem B 110:2180–2186
17. Bujdák J, Iyi N, Sasai R (2004) J Phys Chem B 108:4470–4477
18. Peyratout CS, Möhwald H, Dähne L (2003) Adv Mater 15:1722–1726
19. Sukhorukov G, Dähne L, Hartmann J, Donath E, Möhwald H (2000) Adv Mater 12:112–115
20. Edris A, Bergnståhl B (2001) Nahrung/Food 45:133–137
21. Mcdonald CJ, Bouck KJ, Chaput AB (2000) Macromolecules 33:1593–1605
22. Scott C, Wu D, Ho CC, Co CC (2005) J Am Chem Soc 127:4160–4161
23. Chern CS, Chen TJ, Liou YC (1998) Polymer 39:3767–3777
24. Takasu M, Shiroya T, Takeshita K, Sakamoto M, Kawaguchi H (2004) Colloid Polym Sci 282:740–746
25. Takasu M, Shiroya T, Takeshita K, Sakamoto M, Kawaguchi H (2003) Colloid Polym Sci 282:119–126
26. Hu ZK, Xue MZ, Zhang Q, Sheng QR, Liu YG (2007) J Appl Polym Sci 107:3036–3041
27. Hu ZK, Xue MZ, Zhang Q, Sheng QR, Liu YG (2008) Dyes Pigm 76:173–178
28. Steiert N, Landfester K (2007) Macromol Mater 292:1111–1125
29. Tiarks F, Landfester K (2001) Macromol Chem Phys 202:51–60
30. Rohatgi KK, Singhal GS (1966) J Phys Chem B 70:1695–1701
31. Hoeben FJM, Jonkheijm P, Meijer EW, Schenning APHJ (2005) Chem Rev 105:1491–1546
32. Zhao X, Zhou SX, Chen M, Wu LM (2009) Dyes Pigm 80:212–218
33. Neumann B (2001) J Phys Chem B 105:8268–8274